NASA TECHNICAL MEMORANDUM

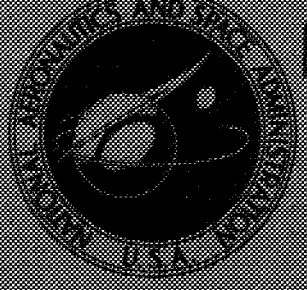

N71-17933

NASA TM X-2193

NASA TM X-2193

CASE FILE COPY

TRANSFER FUNCTION DETERMINATION OF THE PRIMARY LOOP OF A CONCEPTUAL NUCLEAR BRAYTON SPACE POWERPLANT

by Edward J. Petrik and Arthur W. Kieffer

Lewis Research Center
Cleveland, Ohio 44135

NATIONAL AERONAUTICS AND SPACE ADMINISTRATION • WASHINGTON, D. C. • MARCH 1971

1. Report No. NASA TM X-2193	2. Government Accession No.	3. Recipient's Catalog No.
4. Title and Subtitle TRANSFER FUNCTION DETERMINATION OF THE PRIMARY LOOP OF A CONCEPTUAL NUCLEAR BRAYTON SPACE POWERPLANT		5. Report Date March 1971 6. Performing Organization Code
7. Author(s) Edward J. Petrik and Arthur W. Kieffer		8. Performing Organization Report No. E-5830 10. Work Unit No. 120-27
9. Performing Organization Name and Address Lewis Research Center National Aeronautics and Space Administration Cleveland, Ohio 44135		11. Contract or Grant No. 13. Type of Report and Period Covered Technical Memorandum
12. Sponsoring Agency Name and Address National Aeronautics and Space Administration Washington, D. C. 20546		14. Sponsoring Agency Code

15. Supplementary Notes

16. Abstract

The primary loop of a conceptual Nuclear Brayton Space Powerplant was described by a set of nonlinear differential equations. The equations were simplified and linearized. A phase variable technique was used to determine the transfer functions for small step input disturbances in each of the following: (1) reactivity, (2) lithium flow rate in primary loop, (3) argon flow rate in power conversion loop. The time response obtained from the transfer functions for the three input disturbances agrees with the time response obtained from the original nonlinear differential equations.

17. Key Words (Suggested by Author(s))	18. Distribution Statement
Space Power Nuclear Systems Controls	Unclassified - unlimited

19. Security Classif. (of this report)	20. Security Classif. (of this page)	21. No. of Pages	22. Price*
Unclassified	Unclassified	45	$3.00

*For sale by the National Technical Information Service, Springfield, Virginia 22151

TRANSFER FUNCTION DETERMINATION OF THE PRIMARY LOOP OF A CONCEPTUAL NUCLEAR BRAYTON SPACE POWERPLANT

by Edward J. Petrik and Arthur W. Kieffer

Lewis Research Center

SUMMARY

A phase variable technique was used to obtain transfer functions of the primary loop of a conceptual nuclear Brayton space powerplant operating at design conditions.

A set of nonlinear differential equations were written describing the transient behavior of the primary loop. These nonlinear differential equations were simplified and linearized about the system design operating point. Transfer functions were obtained for the primary loop from the linear differential equations for small step input disturbances in each of the following: (1) a 1 cent step reactivity insertion, (2) a 25 percent step in lithium flow rate in the primary loop, (3) a 5 percent step in argon flow rate in the power conversion loop.

A digital computer simulation was used to determine the time response for the three input disturbances of (1) the original nonlinear differential equations, (2) the simplified nonlinear differential equations, (3) the linearized differential equations, (4) and the transfer functions. The results show that the time response obtained from the original equations agree with the time response obtained from the transfer functions.

INTRODUCTION

In the coming years, the electric power requirements for the Nation projected space programs will continue to increase. To meet these projected requirements, the Lewis Research Center has been participating in a technology program aimed at the design of a relatively high-powered nuclear Brayton space powerplant.

The heat source being considered for the Brayton cycle space powerplant is a compact, fast-spectrum nuclear reactor. The design thermal output of the reactor is 2.17 megawatts, and the design operating lifetime for the reactor and powerplant has been set at 50 000 hours.

An area of concern in the overall design of this powerplant is the design of the controls. Analysing the requirements of a closed-loop control system requires the ability to predict the system performance. This ability and the precision of the results depend on how well the characteristics of each component can be expressed mathematically.

One cannot intelligently undertake the design of any closed-loop system without a knowledge of the open-loop transfer function. In this report, the detailed nonlinear differential equations representing the primary loop of a conceptual nuclear Brayton space powerplant are simplified and linearized with respect to three input disturbances. The input disturbances considered are step changes in (1) reactivity (2) lithium flow rate in the primary loop (3) argon flow rate in the power conversion loop. From these simple linear equations, a phase variable or an indirect matrix technique (ref. 1) is used to transform the differential equations into phase variable form. From the phase variable representation, the transfer functions are directly determined.

SYSTEM DESCRIPTION

The equations used to simulate the primary loop of a conceptual nuclear Brayton space powerplant on an analog computer are presented in reference 2. In this section, the primary loop of a nuclear Brayton space powerplant will be briefly described and the equations used in the simulation will be presented.

A simplified sketch of the primary loop of the conceptual nuclear Brayton space powerplant is shown in figure 1. The primary loop is coupled to the gas power conversion loop by a counterflow heat exchanger. The coolant in the primary loop is liquid lithium, and the working fluid in the gas power conversion loop for this study is argon. The design point operating conditions for the primary loop of the nuclear Brayton space powerplant are listed in table I.

Reactor Description

The reactor core has 253 cylindrical fuel pins, each with a diameter of 3/4-inch (1.905 cm) and a length of 14.8 inches (37.6 cm). The pins are made of uranium nitride and are clad with a tantalum alloy with a tungsten liner between fuel and clad. The interior of each fuel pin has a central void. The pins in the assembly are cooled by lithium which flows through annular flow passages formed by the outside surfaces of the fuel pins and the inside surfaces of the surrounding tantalum tubes. The tantalum tubes have an inside diameter of 0.830 inch (2.11 cm). The reactor power is regulated by six control drums which, when rotated, move fuel (or poison) in or out of the core region.

The model used to represent the core consists of a single fuel pin with the composition and dimensions given previously. For calculation purposes, the fuel pin model was divided into three axial segments of equal length. Each segment, consisting of fuel, cladding, the lithium coolant, is described by its proper heat transfer equation. A sketch of the single fuel pin model of the core is shown in figure 2.

Core Analytical Equations

The equations used to simulate the reactor core are described briefly in this section.

Core kinetics. - The reactor thermal power is determined from the following equation:

$$\frac{\bar{dQ}}{dt} = \left(\frac{\delta k - \beta}{l^*}\right) + \sum_{i=1}^{6} \lambda_i D_i \tag{1}$$

(All symbols are defined in appendix A.)

As indicated by equation (1), six delayed neutron groups were considered.

The rate of change in concentration of the delayed-neutron precursors is given by

$$\frac{dD_i}{dt} = \frac{\beta_i}{l^*} Q - \lambda_i D_i \tag{2}$$

The decay constants and yield fractions of the precursors for the six delay groups are listed in table II. The prompt neutron generation time, l^*, is 4.0×10^{-8} seconds.

Reactivity. - The reactivity feedback equations include three separate feedback effects. They are (1) the Doppler coefficient for the reactor fuel and cladding (2) the core geometric expansion temperature coefficient, and (3) the density temperature coefficient for the lithium coolant.

The reactivity feedbacks due to the Doppler effect, the core expansion, and the lithium density change were calculated from the following equations:

$$\frac{d(\delta k_D)}{dT} = \frac{d(\delta k_{D,F})}{dT_{F,av}} + \frac{d(\delta k_{D,K})}{dT_{K,av}} = \frac{2.17\times10^{-4}}{T_{F,av}} - 0.006466\, T_{K,av}^{-0.8} \tag{3}$$

$$\frac{d(\delta k_e)}{dT_{L,av}} = -5.69\times10^{-6} \tag{4}$$

$$\frac{d(\delta k_\rho)}{dT_{L,av}} = -1.627 \tag{5}$$

The terms $T_{F,av}$, $T_{K,av}$, and $T_{L,av}$ in equations (3) and (4) represent the average temperatures of the fuel, cladding, and lithium in the core, respectively. These average temperatures were determined by weighting the respective temperatures in each axial segment of the core in proportion to an assumed axial power distribution.

The axial power distribution was obtained from a digital calculation at the design operating point. The shape of the axial power distribution at the design point resembles a chopped cosine. The shape of the axial distribution was assumed to remain the same at all thermal power levels. The power in the three axial segments of the core was distributed such that about 39.0 percent was produced in the middle segment (segment 2) and about 30.5 percent was produced in each of the other two segments (segments 1 and 3).

Core heat-transfer. - The heat transfer equations for the core, based on a single fuel pin model, are presented below.

The fuel temperature in each axial segment of the core was determined from the equation

$$\frac{d\bar{T}_F}{dt} = \frac{k_{F,av} A_{m,F}}{(\rho V C_p)_F} \frac{\bar{T}_K - \bar{T}_F}{\Delta r_F} + \frac{KQ}{(\rho V C_p)_F} \tag{6}$$

and the cladding temperature was determined from the equation

$$\frac{d\bar{T}_K}{dt} = \frac{k_{K,av} A_{m,K}}{(\rho V C_p)_K} \frac{\bar{T}_F - \bar{T}_K}{\Delta r_K} + \frac{h_{L,C} S_C (\bar{T}_L - \bar{T}_K)}{(\rho V C_p)_K} \tag{7}$$

The lithium temperature in each axial core segment was determined from

$$\frac{d\bar{T}_{L,C}}{dt} = \left(\frac{\dot{W}}{\rho A}\right)_L \frac{\Delta T_{L,C}}{\Delta X_C} + \frac{h_{L,C} S_C}{(\rho V C_p)_L} (\bar{T}_L - \bar{T}_K) \tag{8}$$

Heat Exchanger Description

Model. - The heat exchanger model described in this section should not be considered as a design configuration. Rather, it is only one of many possible conceptual

configurations capable of transferring the heat load from the primary loops to the gas-power conversion loop.

A counterflow shell-and-tube type heat exchanger was assumed for the simulation. The conceptual heat exchanger has 331 circular tubes; the tubes have an inside diameter of 3/4-inch (1.905 cm), a wall thickness of 0.05 inch (0.127 cm) and a length of approximately of 8 feet (2.44 m).

Argon gas is assumed to flow inside the tubes, and lithium flows countercurrently in the shell. The heat exchanger tubes are arranged in a hexagonal cross sectional array.

The model for the counterflow heat exchanger simulation is a single tube with argon flowing inside the tube and lithium flowing countercurrently on the outside. The model was considered to be made up of three axial segments of equal length. Figure 3 is a sketch of the heat exchanger model.

Heat-exchanger equations. - The heat transfer equations used in the simulation of the heat exchanger are described briefly below.

The lithium temperature in each heat exchanger segment was computed from the equation

$$\frac{d\bar{T}_{L,HX}}{dt} = \frac{\dot{W}_L}{\rho_L A_L}\frac{\Delta T_{L,HX}}{\Delta X_{HX}} + \frac{h_{L,HX} S_{L,HX}}{\rho_L V_L C_{p,L}}\left(\bar{T}_{W,HX} - \bar{T}_{L,HX}\right) \tag{9}$$

And the wall temperature for each segment of the heat exchanger was computed from the equation

$$\frac{d\bar{T}_{W,HX}}{dt} = \frac{h_{L,HX} S_{L,HX}}{(\rho V C_p)_W}\left(\bar{T}_{L,HX} - \bar{T}_{W,HX}\right) + \frac{h_g S_{g,HX}}{(\rho V C_p)_W}\left(\bar{T}_g - \bar{T}_{W,HX}\right) \tag{10}$$

The temperature of the argon gas in each axial segment was computed from the equation

$$\frac{dT_g}{dt} = \frac{1}{\rho_g}\left[\frac{\dot{W}_g}{A_g}\frac{\Delta T_{g,HX}}{\Delta X_{HX}} + \frac{h_g S_{g,HX}}{V_g C_{p,g}}\left(\bar{T}_{W,HX} - \bar{T}_g\right)\right] \tag{11}$$

Heat-Transfer Coefficients

The liquid metal heat transfer coefficient for the reactor core was calculated from the equation

$$Nu_{L,C} = 5.591 + 4.595\times10^{-4}\left(Re_{L,C}\right)^{0.7998} \tag{12}$$

And the liquid metal heat transfer coefficient for the heat exchanger was calculated from the equation

$$Nu_{L,HX} = 8\left(Pe_{L,HX}\right)^{0.6}\left[\left(\frac{D_H}{L}\right)_{L,HX} + 0.027\left(\frac{S}{d} - 1.111\right)\right]^{0.046} \tag{13}$$

The film coefficient on the gas side of the heat exchanger was calculated from the Dittus-Boelter expression:

$$Nu_g = 0.023\left(Re_g\right)^{0.8}\left(Pr_g\right)^{0.4} \tag{14}$$

Transport Lag Representation

In the primary loop of the nuclear Brayton space powerplant, the transport lag (or time delay) is defined as the average time required for the coolant to traverse the loop. However, it is assumed that the heat exchanger is close coupled to the reactor such that nearly all of the time delay occurs in the heat exchanger. Because of this, only the transport lag in the heat exchanger was considered. Thus, the fluid temperatures at the inlet of each of the three heat exchanger segments were delayed by one-third of the delay time before entering the next heat exchanger segment.

At the design lithium flow rate, the time delay is about 10 seconds. Therefore, a change in the lithium temperature at the reactor outlet goes unnoticed at the reactor inlet for about 10 seconds. For lithium flow rates of 50 percent and 10 percent of the design value, the time delays would be about 20 seconds and 100 seconds, respectively.

It should be recognized that these time delays are primarily a characteristic of the heat exchanger design used in the simulation. These time delays may change with the heat exchanger design configuration.

ANALYSIS

Analysis of a dynamic system requires the ability to predict the systems performance. The ability and precision of the results depend on how well the characteristics of each component can be expressed mathematically. In the previous section, the equations (ref. 2) used to simulate the nuclear Brayton space powerplant on an analog computer

were presented. In this section the nonlinear differential equations will be simplified and then linearized about the design operating point of the nuclear Brayton space powerplant (NBSP). Transfer functions will be derived from the linear differential equations for small step input disturbances.

Simplifying the Brayton System Equations

In general, three simplifying assumptions will be used to reduce the number of nonlinear differential equations which describe the NBSP.

The first assumption considered is related to equation (1). As indicated, six delayed neutron groups were considered in the original simulation. It will be assumed that there is only one group of delayed neutrons. And the decay constant is equal to a properly weighted average of the six actual groups (ref. 3).

The decay constant is computed as follows

$$\lambda = \frac{\beta}{\sum_{i=1}^{6} \frac{\beta_i}{\lambda_i}} = 7.85\times10^{-2}\ \text{sec}^{-1} \tag{15}$$

The next simplification considers one axial segment (lump) for both the reactor and heat exchanger. Originally, each model was divided into three axial segments or lumps.

Because the reactor heat transfer equations will now consist of one axial segment, the calculated fuel and cladding temperature will represent the average fuel and cladding temperature. Thus, the terms $T_{F,av}$ and $T_{K,av}$ in the reactivity feedback (eqs. (3) and (4)) will be T_F and T_K. In addition, the average temperature of the lithium in the core for the reactivity feedback will be determined by averaging the reactor inlet and reactor exit lithium temperature. This is expressed by equation (16).

$$T_{L,av} = \frac{T_{L,out} + T_{L,in}}{2} \tag{16}$$

Finally, it is assumed that the reactor cladding temperature is equal to the lithium temperature in the core. And the wall temperature of the heat exchanger is equal to the lithium temperature in the heat exchanger. This assumption is valid for step disturbances in reactivity and argon flow rate since the resistance to heat transfer between the cladding and liquid or liquid to heat exchanger wall is negligible. That is, the liquid

metal heat transfer coefficient is extremely large. Therefore, an overall heat transfer coefficient is used in the simplified nonlinear differential equations.

For a step disturbance of lithium flow rate the preceding assumption that the reactor cladding temperature is equal to the liquid lithium temperature in the core is valid. However, the wall temperature associated with the lithium temperature at the heat exchanger exit is not negligible. Thus, the heat exchanger wall temperature will be included in the simplified nonlinear differential equations.

Applying the above simplifications to the original nonlinear differential equations reduces the number of equations from 25 to 5 for step disturbances of reactivity and argon flow rates. And reduces the number of equations from 25 to 6 for a step disturbance of lithium flow rate. Appendix B presents the final simplified nonlinear equations.

Linear Brayton System Equations

The set of simultaneous nonlinear differential equations as derived are linearized in this section. These equations are expressed as five first-order equations of the form

$$\frac{d\hat{X}}{dt} = \hat{f}(\hat{X}, \hat{u}) \tag{17}$$

where $\hat{u}$ is the input. The shorthand notation for the column vector is a $\hat{}$ as example

$$\hat{X} = \begin{bmatrix} x_1 \\ x_2 \\ -- \\ -- \\ -- \\ x_n \end{bmatrix} = \text{col}(x_1, x_2, \ \cdots \ x_n) \tag{18}$$

To find a linear approximation of the nonlinear equations, the equations must be linearized about some operating point. The solutions are then valid only in a neighborhood of the point.

The equations are linearized by expanding $\hat{f}(\hat{X}, \hat{u})$ in a Taylor series (ref. 4) about the operating point $\hat{X}^o$ and $\hat{u}^o$, as follows

$$\hat{f}(\hat{X}, \hat{u}) = \hat{f}(\hat{X}^o, \hat{u}^o) + \frac{\partial \hat{f}(\hat{X}, \hat{u})}{\partial \hat{X}} \Bigg|_{\substack{\hat{X}=\hat{X}^o \\ \hat{u}=\hat{u}^o}} (\hat{X} - \hat{X}^o) + \frac{\partial \hat{f}(\hat{X}, \hat{u})}{\partial \hat{u}} \Bigg|_{\substack{\hat{X}=\hat{X}^o \\ \hat{u}=\hat{u}^o}} (\hat{u} - \hat{u}^o) + \text{higher-order terms} \tag{19}$$

Let $\hat{X}^* = \hat{X} - \hat{X}^o$ and $\hat{u}^* = \hat{u} - \hat{u}^o$ be the changes in $\hat{X}$ and $\hat{u}$ from the operating point $\hat{X}^o$ and $\hat{u}^o$. Since $\hat{X}^o$ and $\hat{u}^o$ are assumed to be equilibrium conditions, $d\hat{X}/dt = d\hat{X}^*/dt$ and $\hat{f}(\hat{X}^o, \hat{u}^o)$ is defined to be 0. Thus, the first-order approximation of

$$\frac{d\hat{X}}{dt} = \hat{f}(\hat{X}, \hat{u}) \tag{20}$$

can be written as

$$\frac{d\hat{X}^*}{dt} = \frac{\partial \hat{f}(\hat{X}, \hat{u})}{\partial \hat{X}}\Bigg|_{\substack{\hat{X}=\hat{X}^o \\ \hat{u}=\hat{u}^o}} \hat{X}^* + \frac{\partial \hat{f}(\hat{X}, \hat{u})}{\partial \hat{u}}\Bigg|_{\substack{\hat{X}=\hat{X}^o \\ \hat{u}=\hat{u}^o}} \hat{u}^* \tag{21}$$

The linearized set of differential equations now take the form

$$\frac{d\hat{X}^*}{dt} = \hat{A}\hat{X}^* + \hat{B}\hat{u}^* \tag{22}$$

where $\hat{A}$ and $\hat{B}$ are matrices, the elements of which are determined from

$$a_{ij} = \frac{\partial f_i(\hat{X}, \hat{u})}{\partial x_j}\Bigg|_{\substack{\hat{X}=\hat{X}^o \\ \hat{u}=\hat{u}^o}} \tag{23}$$

and

$$b_{ij} = \frac{\partial f_i(\hat{X}, \hat{u})}{\partial u_j}\Bigg|_{\substack{\hat{X}=\hat{X}^o \\ \hat{u}=\hat{u}^o}} \tag{24}$$

The linearization procedure as described above assumes that the vector function is continuously differentiable in all its arguments. Two variables, the transport delay and the heat transfer coefficients on the gas side of the heat exchanger, are not continuously differentiable.

The transport delay will be approximated by using a second-order Padé approximation given in reference 5. A higher order approximation could be used except that the number of differential equations needed for the approximation is equal to the order of the approximation. Thus, the transport delay $y = x$ where x is delayed by τ seconds is given as follows.

$$\frac{du}{dt} = v - \frac{12}{\tau} x \tag{25}$$

$$\frac{dv}{dt} = -\frac{12}{\tau^2} u - \frac{6}{\tau} v + \frac{72}{\tau^2} x \tag{26}$$

$$y = u + x \tag{27}$$

The heat transfer coefficient is a discrete function of the gas temperature given in tabular form. A least-square quadric curve fit was used to make the heat transfer coefficient a continuous function of gas temperature without increasing the number of differential equations.

Appendix C presents the detailed linearization as described previously for reactivity and argon flow rate disturbances. The linearization procedure for lithium flow rate disturbances is the same as appendix C except the nonlinear differential equations include the heat exchanger wall temperature.

Transfer Functions

If a system is linear and time invariant, the transfer function conveniently relates the response of the system to a forcing function with the aid of appropriate Laplace transforms. If R(S) represents the Laplace transform of the input disturbance, C(S) represents the transform of the response, and G(S) represents the transfer function, then

$$C(S) = R(S)G(S) \tag{28}$$

or

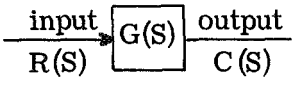

In the preceding equation or diagram it is assumed that the system is initially at rest, that is, all initial conditions are equal to zero.

Since the equations representing the nuclear Brayton space powerplant derived in the previous section are linear differential equations with constant coefficients, the basic problem associated with determining the transfer functions is solving the equations only in terms of the output and input variable. This becomes tedious if the order is greater than two.

Block diagram manipulation can also be used to find the transfer functions. Unfortunately, this also becomes laborious if there are many internal feedback loops such as the reactivity feedback in the NBSP.

The method used in this report is referred to as the indirect matrix or phase variable approach. This method is based on the realization that, if the system is transformed into phase variables, the transfer functions may be determined by inspection. In addition to determining an overall transfer function, any number of internal transfer function may be determined at the same time. Reference 1 formulates the indirect matrix method and describes a digital program implementing the method.

The indirect matrix or phase variable method was applied to the linear differential equation to obtain the transfer functions. The list of transfer functions in both polynomial and factored forms of the Laplace transform variable s for the three input disturbance follow:

Input disturbance in reactivity. -

Denominator:

$$D(s) = s^7 + 33.3\,s^6 + 224.5\,s^5 + 224.7\,s^4 + 102.5\,s^3 + 27.0\,s^2 + 0.494\,s + 0.01493$$

or

$$s_1, s_2 = -8.653\times10^{-3} \pm 2.277\times10^{-2}\,j$$

$$s_3, s_4 = -0.2288 \pm 0.4005\,j$$

$$s_5 = -0.6279$$

$$s_6 = -7.688$$

$$s_7 = -24.51$$

Numerator:

(1) Concentration of delayed-neutron precursors

$$\frac{C(s)}{\rho_{in}(s)} = \frac{F_c N_1(s)}{D(s)}$$

$$N_1(s) = [1.341\,s^6 + 44.67\,s^5 + 300.8\,s^4 + 294.0\,s^3 + 130.4\,s^2 + 34.65\,s + 0.3239]\times10^4$$

or

$$s_1, s_2 = -0.2151 \pm 0.4016\,j$$

$$s_3 = -0.6344$$

$$s_4 = -0.9693 \times 10^{-2}$$

$$s_5 = -7.718$$

$$s_6 = -24.51$$

(2) Reactor fuel temperature

$$\frac{T_F(s)}{\rho_{in}(s)} = \frac{N_2(s)}{D(s)}$$

$$N_2(s) = 0.8032\,s^6 + 26.13\,s^5 + 162.5\,s^4 + 115.7\,s^3 + 46.15\,s^2 + 4.811\,s + 0.1409$$

or

$$s_1, s_2 = -0.3096 \pm 0.3704\,j$$

$$s_3 = -0.7854 \times 10^{-1}$$

$$s_4 = -0.5383 \times 10^{-1}$$

$$s_5 = -7.266$$

$$s_6 = -24.51$$

(3) Reactor exit lithium temperature

$$\frac{T_{L,C}(s)}{\rho_{in}(s)} = \frac{N_3(s)}{D(s)}$$

$$N_3(s) = 2.963\,s^5 + 75.13\,s^4 + 62.43\,s^3 + 20.63\,s^2 + 2.838\,s + 0.1256$$

or

$$s_1, s_2 = -0.2879 \pm 0.1647\ j$$

$$s_3 = -0.8303 \times 10^{-1}$$

$$s_4 = -0.1893$$

$$s_5 = -24.51$$

(4) Heat exchanger exit lithium temperature

$$\frac{T_{L,HX}(s)}{\rho_{in}(s)} = \frac{N_4(s)}{D(s)}$$

$$N_4(s) = 0.4969\ s^4 + 11.94\ s^3 - 5.972\ s^2 + 0.7833\ s + 0.1041$$

or

$$s_1, s_2 = 0.2857 \pm 0.1650\ j$$

$$s_3 = -0.7854 \times 10^{-1}$$

$$s_4 = -24.51$$

(5) Argon gas temperature

$$\frac{T_g(s)}{\rho_{in}(s)} = \frac{N_5(s)}{D(s)}$$

$$N_5(s) = 57.21\ s^4 + 48.53\ s^3 + 16.17\ s^2 + 2.232\ s + 0.9694 \times 10^{-1}$$

or

$$s_1, s_2 = -0.2857 \pm 0.1650\ j$$

$$s_3 = -0.1982$$

$$s_4 = -0.7854 \times 10^{-1}$$

Input disturbance in argon flow rate. -

Denominator:

$$D(s) = s^7 + 34.47\, s^6 + 234.7\, s^5 + 235.2\, s^4 + 107.2\, s^3 + 28.17\, s^2 + 0.5262\, s + 0.1554\times10^{-1}$$

or

$$s_1, s_2 = -\, 0.8875\times10^{-2} \pm 0.2267\times10^{-1}\, j$$

$$s_3, s_4 = -\, 0.2292 \pm 0.3991\, j$$

$$s_5 = -\, 0.6270$$

$$s_6 = -\, 7.687$$

$$s_7 = -\, 25.68$$

Numerator:

(1) Concentration of delayed-neutron precursors

$$\frac{C(s)}{\dot{W}_g(s)} = \frac{F_C N_1(s)}{D(s)}$$

$$N_1(s) = [12.78\, s^5 + 499.2\, s^4 + 4573.0\, s^3 + 4793.0\, s^2 + 1774.0\, s + 248.9]\times10^{-4}$$

or

$$s_1, s_2 = -\, 0.2857 \pm 0.1650\, j$$

$$s_3 = -\, 0.5697$$

$$s_4 = -\, 12.23$$

$$s_5 = -\, 25.68$$

(2) Reactor fuel temperature

$$\frac{T_F(s)}{\dot{W}_g(s)} = \frac{N_2(s)}{D(s)}$$

$$N_2(s) = 7.655\ s^5 - 217.4\ s^4 - 0.1086\times10^5\ s^3 - 5973.0\ s^2 - 1063.0\ s + 20.07$$

or

$$s_1, s_2 = -0.2857 \pm 0.1650\ j$$

$$s_3 = 0.1718\times10^{-1}$$

$$s_4 = -25.68$$

$$s_5 = 54.63$$

(3) Reactor exit lithium temperature

$$\frac{T_{L,C}(s)}{\dot{W}_g(s)} = \frac{N_3(s)}{D(s)}$$

$$N_3(s) = -598.4\ s^5 - 0.1619\times10^5\ s^4 - 0.2148\times10^5\ s^3 - 8729.0\ s^2 - 1312.0\ s + 6.348$$

or

$$s_1, s_2 = -0.2857 \pm 0.1650\ j$$

$$s_3 = 0.4690\times10^{-2}$$

$$s_4 = -0.8093$$

$$s_5 = -25.68$$

(4) Heat exchanger exit lithium temperature

$$\frac{T_{L,HX}(s)}{\dot{W}_g(s)} = \frac{N_4(s)}{D(s)}$$

$$N_4(s) = -[171.4\ s^6 + 5891.0\ s^5 + 0.3928\times10^5\ s^4 + 0.3524\times10^5\ s^3 + 0.1203\times10^5\ s^2 +$$

$$1574.0\ s + 8.198]$$

or

$$s_1, s_2 = -0.2857 \pm 0.1650\ j$$

$$s_3 = -0.5430 \times 10^{-2}$$

$$s_4 = -0.4134$$

$$s_5 = -7.602$$

$$s_6 = -25.68$$

(5) Argon gas temperature

$$\frac{T_g(s)}{\dot{W}_g(s)} = \frac{N_5(s)}{D(s)}$$

$$N_5(s) = -[16.82\ s^6 + 147.9\ s^5 + 163.4\ s^4 + 86.03\ s^3 + 25.23\ s^2 + 1.37\ s + 0.5216 \times 10^{-2}]\ 10^3$$

or

$$s_1, s_2 = -0.2569 \pm 0.4370\ j$$

$$s_3 = -0.4111 \times 10^{-2}$$

$$s_4 = -0.6308 \times 10^{-1}$$

$$s_5 = -0.6123$$

$$s_6 = -7.597$$

Input disturbance in lithium flow rate. -

Denominator:

$$D(s) = s^8 + 56.17\ s^7 + 1001.0\ s^6 + 5759.0\ s^5 + 6317.0\ s^4 + 3152.0\ s^3 + 804.0\ s^2 + 12.27 + 0.3609$$

or

$$s_1, s_2 = -0.7139\times10^{-3} \pm 0.2063\times10^{-1}\ j$$

$$s_3, s_4 = -0.2940 \pm 0.4125\ j$$

$$s_5 = -0.6473$$

$$s_6 = -8.465$$

$$s_7 = -22.28$$

$$s_8 = -24.17$$

Numerator:

(1) Concentration of delayed-neutron precursors

$$\frac{C(s)}{\dot{W}_L(s)} = \frac{F_C \cdot N_1(s)}{D(s)}$$

$$N_1(s) = [4.235\ s^6 + 203.0\ s^5 + 2574.0\ s^4 + 3460.\ s^3 + 1324\ s^2 + 43.79\ s - 0.0289]\times10^6$$

or

$$s_1, s_2 = -0.7145 \pm 0.1242\ j$$

$$s_3 = 0.6471\times10^{-3}$$

$$s_4 = -0.3718\times10^{-1}$$

$$s_5 = -22.31$$

$$s_6 = -24.17$$

(2) Reactor fuel temperature

$$\frac{T_F(s)}{\dot{W}_L(s)} = \frac{N_2(s)}{D(s)}$$

$$N_2(s) = -[0.2091\times10^{-2}\, s^7 + 3.474\, s^6 + 160.3\, s^5 + 1931\, s^4 + 1342\, s^3 + 339.0\, s^2 + 4.525\, s + 0.151]10^3$$

or

$$s_1, s_2 = -\,0.6064\times10^{-2} \pm 0.2079\times10^{-1}\, j$$

$$s_3, s_4 = -\,0.3553 \pm 0.2261\, j$$

$$s_5 = -\,22.26$$

$$s_6 = -\,24.17$$

$$s_7 = -\,1614.0$$

(3) Reactor exit lithium temperature

$$\frac{T_{L,C}(s)}{\dot{W}_L(s)} = \frac{N_3(s)}{D(s)}$$

$$N_3(s) = -[4.23\, s^7 + 203.2\, s^6 + 2590.\, s^5 + 3745.\, s^4 + 1843.\, s^3 + 352.7\, s^2 + 4.911\, s + 0.1500]\times10^3$$

or

$$s_1, s_2 = -\,0.6224\times10^{-2} \pm 0.2043\times10^{-1}\, j$$

$$s_3, s_4 = -\,0.3571 \pm 0.2062\, j$$

$$s_5 = -\,0.8486$$

$$s_6 = -\,22.26$$

$$s_7 = -\,24.17$$

(4) Heat exchanger exit lithium temperature

$$\frac{T_{L,HX}(s)}{\dot{W}_L(s)} = \frac{N_4(s)}{D(s)}$$

$$N_4(s) = [0.1152\ s^7 + 5.811\ s^6 + 90.08\ s^5 + 437.8\ s^4 + 715.9\ s^3 + 416.6\ s^2 + 6.664\ s + 0.2020]\times 10^3$$

or

$$s_1, s_2 = -0.7785\times 10^{-2} \pm 0.2092\times 10^{-1}\ j$$

$$s_3, s_4 = -1.188 \pm 0.4929\ j$$

$$s_5 = -4.555$$

$$s_6 = -19.33$$

$$s_7 = -24.17$$

(5) Argon gas temperature

$$\frac{T_g(s)}{\dot{W}_L(s)} = \frac{N_5(s)}{D(s)}$$

$$N_5(s) = [3.103\ s^7 + 17.85\ s^6 - 1234.\ s^5 - 2126.\ s^4 - 1055.\ s^3 - 177.4\ s^2 - 2.330\ s - 0.7302\times 10^{-1}]10^3$$

or

$$s_1, s_2 = -0.5685\times 10^{-2} \pm 0.2027\times 10^{-1}\ j$$

$$s_3, s_4 = -0.3465 \pm 0.1082\ j$$

$$s_5 = -0.9938$$

$$s_6 = 18.21$$

$$s_7 = -22.27$$

Of special significance is the order of the characteristic equations for the various disturbances. For a lithium flow rate disturbance, the characteristic equation is eighth-order whereas the characteristic equation is seventh-order for reactivity and argon flow rate disturbance.

RESULTS

In this section, the time response of the reactor exit lithium temperature to a step disturbance in (1) reactivity, (2) argon flow rate, and (3) lithium flow rate will be described. The time response was determined by digital computer using the continuous system modeling program. The step disturbances were imposed with the nuclear Brayton space powerplant operating at design (table I).

As stated in the ANALYSIS section, the original nonlinear differential equations (ref. 1) were simplified and linearized before obtaining the transfer functions. To show the effects of the assumptions, the time response of the reactor exit lithium temperature will be presented at each step of the simplification. The assumptions used are described and referred to as case A to D in table III.

Step Change in Reactivity

With the nuclear Brayton space powerplant at the steady-state design point, a positive step change in reactivity of one cent was made. As a result, the thermal power output of the reactor changes and the lithium temperature at the reactor exit changes with time as shown in figure 4.

In what follows, the difference in time response of the reactor exit lithium temperature will be described by pointing out the effects of the simplifying assumptions.

Figure 4(a) is a plot of the time response for the original simulation. A peak temperature change of about 9.5 ^{o}R (5.3 K) is reached in approximately 125 seconds. Figure 4(b) is the time response of the reactor exit lithium temperature for case A. In this figure, a peak temperature change of approximately 11^{o} R (6.1 K) is reached in about 150 seconds. The difference in the time response can be minimized by using some other approximate formulation of the six-group delayed neutron. However, for a closed-loop control this difference may be considered negligible.

Cases B and C are now considered by comparing figures 4(c) and (d) with 4(a). The difference in the time at which the peak temperature occurs as compared with figure 4(a) is less than 10 seconds. In addition, the difference in the peak value is less than 2^{o} R (1.1 K). The difference in the peak value and the time at which it occurred can be considered negligible.

Figures 4(e) and (f) are plots of the time response of the reactor exit lithium temperature for the linear differential equations and its corresponding transfer function. Comparing these figures with figure 4(a) shows that the transfer function approximates the reactor exit lithium temperature.

Step Change in Argon Flow Rate

With the system operating at design conditions, a 5-percent step increase is made in the argon flow rate. This increase in argon flow rate directly affects the system in two ways. It reduces the dwell time of the gas in the heat exchanger and it also improves the gas heat transfer coefficient.

Figure 5(a) is a plot of the lithium temperature at the reactor exit for the original simulation. The reactor exit temperature decreases during the initial 50 seconds because more heat is transferred to the gas in the heat exchanger.

Figures 5(b) to (d) are plots of the time response of the reactor exit lithium temperature for case A to C. Comparing these figures with figure 5(a) also shows that the simplifying assumptions are valid as they were for the reactivity disturbance described previously. In addition, the transfer function approximates the reactor exit lithium temperature for a step disturbance in argon flow rate since figures 5(e) and (f) compares with figure 5(a).

Step Change in Lithium Flow Rate

With the NBSP at steady-state design conditions, a step increase of 25 percent was made in the lithium flow rate. A large step in lithium flow rate was chosen because the liquid lithium flow rate effects on the NBSP are rather insensitive. This behavior is explained in detail in reference 2.

The time response of the reactor exit lithium temperature to the step in lithium flow rate for the original simulation is shown in figure 6(a).

The immediate effect of this disturbance is an increase in the lithium velocity through the reactor and heat exchanger. This velocity increase has little effect on the lithium heat transfer coefficient. However, it does reduce the lithium dwell time in the reactor and heat exchanger. As a result, the lithium loses less heat in the heat exchanger and also gains less heat in the reactor. Therefore, the lithium temperature at the reactor exit immediately decreases approximately 14^{o} R (7.8 K) during the initial 3 seconds as shown in figure 6(a).

The time response of the reactor exit lithium temperature for cases A, B, and D are shown in figures 6(b) to (d). The initial peak occurs during the first 3 seconds (the same as in fig. 6(a)). And the peak values for figures 6(a) to (d) are within 2^{o} R (1.1 K).

Figure 6(e) and (f) are plots of the time response of the reactor exit lithium temperature for the linear differential equations and its corresponding transfer function. Comparing these figures with figure 6(a) again shows that the transfer function approximates the reactor exit lithium temperature of the original simulation.

In the foregoing discussion, only the time response of the reactor exit lithium temperature to an input disturbance was described. This showed the step by step procedure that was used to obtain the different transfer functions which relate the reactor exit lithium temperature to the different input disturbances. In table IV, we have summarized the time response of the major variables comparing the original simulation and the transfer function approximation.

Of special significance in table IV is the time of the peak overshoot. With the NBSP initially at its steady-state design point, the time of peak overshoot for a reactivity step insertion of 1 cent is about 125 seconds. For a 5-percent step in argon flow rate, the time of peak overshoot is about 70 seconds. In contrast, a 25-percent step disturbance in lithium flow rate, the time of peak overshoot is less than 12 seconds. Hence, the response of the system to an input disturbance in flow rate is extremely fast.

SUMMARY OF RESULTS

The transfer functions representing the primary loop of a conceptual nuclear Brayton space powerplant operating at design power were determined for three input disturbances. The input disturbances included (1) a 1 cent step of reactivity, (2) a 5-percent step of argon flow rate in power conversion loop, and (3) a 25-percent step of lithium flow rate in primary loop.

The primary loop was described by a set of nonlinear differential equations. These equations were simplified and linearized about the design power operating point. The transfer functions were obtained from the linear differential equations by using an indirect matrix or phase variable method.

A digital computer simulation was used to determine the time responses of the original nonlinear differential equations and of the transfer functions. The results indicate that the transfer functions do represent the primary loop of a conceptual nuclear Brayton space powerplant.

Lewis Research Center,
National Aeronautics and Space Administration,
Cleveland, Ohio, October 29, 1970,
120-27.

APPENDIX A

SYMBOLS

A	flow area, ft^2; m^2
$\hat{A}$	coefficient matrix
A_m	mean heat conduction area, ft^2; m^2
a_{ij}	matrix elements
$\hat{B}$	column matrix
b_j	elements of column matrix
C	concentrations of delayed neutron precursors in the i^{th} group
C_p	specific heat at constant pressure, Btu/(lbm)(^oR); (kW)(sec)/(Rg)(K)
D_H	hydraulic diameter, ft; m
D_i	contribution to power from i^{th} group of delayed neutron precursors
d	outside diameter of tubes in heat exchanger, ft; m
F_C	proportionality constant, Btu(cm^3)/neutrons sec; (kW)(cm^3)/neutrons
$\hat{f}(\ )$	matrix function of
h	heat transfer coefficient, Btu/(sec)(ft^2)(^oR); kW/(m^2)(K)
K	fraction of total power generated in fuel section
k	thermal conductivity, Btu/(ft)(sec)(^oR); kW/(m)(K)
L	length, parallel to flow, ft; m
ℓ^*	prompt neutron generation time, sec
Nu	Nusselt number
Pe	Peclet number
Pr	Prandtl number
Q	reactor power, Btu/sec; kW
Re	Reynolds number
Δr	incremental distance in a direction radial to flow, ft; m
S	heat transfer area, ft^2; m^2
s	Laplace transform variable
T	temperature, ^oR; K
$\bar{T}$	average section temperature, ^oR; K
ΔT	temperature increment, ^oR; K
t or τ	time, sec
U	overall heat transfer coefficient, Btu/(sec)(ft^2)(^oR); kW/(m^2)(K)
u	independent variable
$\hat{u}$	column vector
u_j	elements of column vector
V	volume, ft^3; m^3
v	independent variable
$\dot{W}$	flow rate, lbm/sec; kg/sec
$\hat{X}$	column vector
ΔX	incremental distance in a direction axial to flow, ft; m
x	independent variable
x_i	elements of column vector
y	dependent variable

β	total delayed neutron precursor yield
β_i	delayed neutron precursor yield fraction in i^{th} group
λ	average delayed neutron precursor decay constant
λ_i	delayed neutron precursor decay constant in i^{th} group
δk	reactivity
ρ	density, lbm/ft^3; kg/m^3
ρ_i	i^{th} constant
ρ_{in}	reactivity insertion

Subscripts:

av	average
C	core
D	pertaining to the Doppler reactivity effect
E	pertaining to the reactivity effect due to core expansion
F	fuel
g	argon gas
HX	heat exchanger
in	inlet or input
K	fuel cladding
L	liquid lithium
W	tube wall in heat exchanger
ρ	pertaining to the reactivity effect due to lithium density change
τ	delayed τ seconds

Superscripts:

0	steady-state operating point
*	change in variable

APPENDIX B

SIMPLIFIED NONLINEAR DIFFERENTIAL EQUATIONS DESCRIBING THE NUCLEAR BRAYTON SPACE POWERPLANT

Equations for Reactivity and Argon Flow Rate Disturbances

Concentration of delayed-neutron precursors:

$$\frac{dD}{dt} = \frac{\beta}{l^*} Q - \lambda D$$

where

$$Q = \frac{l^* \lambda D}{\beta - \delta k}$$

Reactor fuel temperature:

$$\frac{dT_F}{dt} = \frac{S_C}{(\rho V C_p)_F} U_{L,C}(T_{L,C} - T_F) + \frac{Q}{(\rho V C_p)_F}$$

Reactor exit lithium temperature:

$$\frac{dT_{L,C}}{dt} = \left(\frac{\dot{W}}{\rho V}\right)_L (T_{L,HX} - T_{L,C}) + \frac{S_C}{(\rho V C_p)_L} U_{L,C}(T_F - T_{L,C})$$

Heat exchanger exit lithium temperature:

$$\frac{dT_{L,HX}}{dt} = \left(\frac{\dot{W}}{\rho A}\right)_{HX} \frac{\Delta T_{L,HX}}{\Delta X_{HX}} + \frac{S_{L,HX}}{(\rho V C_p)_L} U_{L,HX}(T_{g,in} - T_{L,HX})$$

and

$$\frac{\Delta T_{L,HX}}{\Delta X_{HX}} \cong K_{K,L}(T_{L,C,\tau} - T_{L,HX})$$

Argon gas temperature:

$$\frac{dT_g}{dt} = \frac{1}{\rho_g}\left[\frac{\dot{W}_g}{A_g}\frac{\Delta T_{g,HX}}{\Delta X_{HX}} + \left(\frac{S}{VC_p}\right)_g U_g(T_{L,C} - T_g)\right]$$

and

$$\frac{\Delta T_{g,HX}}{\Delta X_{HX}} \cong K_{K,g}(T_{g,in} - T_g)$$

Equations for Lithium Flow Rate Disturbance

Concentration of delayed-neutron precursors:

$$\frac{dD}{dt} = \frac{\beta}{l^*}Q - \lambda D$$

where

$$Q = \frac{l^*\lambda D}{\beta - \delta k}$$

Reactor fuel temperature:

$$\frac{dT_F}{dt} = \frac{S_C}{(\rho VC_p)_F}U_{L,C}(T_{L,C} - T_F) + \frac{Q}{(\rho VC_p)_F}$$

Reactor exit lithium temperature:

$$\frac{dT_{L,C}}{dt} = \left(\frac{\dot{W}}{\rho V}\right)_L (T_{L,HX} - T_{L,C}) + \frac{S_C}{(\rho VC_p)_L}(T_F - T_{L,C})$$

Heat exchanger exit lithium temperature:

$$\frac{dT_{L,HX}}{dt} = \left(\frac{\dot{W}}{\rho A}\right)_{HX} \frac{\Delta T_{L,HX}}{\Delta X_{HX}} + \frac{S_{L,HX}}{(\rho V C_p)_L} h_{L,HX}(T_W - T_{L,HX})$$

and

$$\frac{\Delta T_{L,HX}}{\Delta X_{HX}} \cong K_{K,L}(T_{L,C,\tau} - T_{L,HX})$$

Argon gas temperature:

$$\frac{dT_g}{dt} = \frac{1}{\rho_g}\left[\frac{\dot{W}_g}{A_g} \frac{\Delta T_{g,HX}}{\Delta X_{HX}} + \left(\frac{S}{VC_p}\right)_g U_g(T_{L,C} - T_g)\right]$$

and

$$\frac{\Delta T_{g,HX}}{\Delta X_{HX}} \cong K_{K,g}(T_{g,in} - T_g)$$

Heat exchanger wall temperature:

$$\frac{dT_W}{dt} = \frac{S_{L,HX}}{(\rho V C_p)_W} h_{L,HX}(T_{L,HX} - T_W) + \frac{S_{g,HX}}{(\rho V C_p)_W} h_{g,in}(T_{G,in} - T_W)$$

APPENDIX C

LINEARIZATION OF THE SIMPLIFIED NONLINEAR DIFFERENTIAL EQUATIONS FOR REACTIVITY AND ARGON FLOW RATE DISTURBANCES

The following equations were presented in appendix B, except that the constant coefficients are now expressed numerically and the variables are expressed in terms of the column vector elements.

Concentration of delayed-neutron precursors:

$$\dot{x}_1 = \lambda\beta(\beta - \delta k)^{-1} x_1 - \lambda x_1$$

Reactor fuel temperature:

$$\dot{x}_2 = 2.398\, U_{L,C}(x_3 - x_2) + 9.88\, \lambda l^*(\beta - \delta k)^{-1} x_1$$

Reactor exit lithium temperature:

$$\dot{x}_3 = 42.5\, \dot{W}(x_4 - x_3) + 10.37\, U_{L,C}(x_2 - x_3)$$

Heat exchanger lithium temperature:

$$\dot{x}_4 = 11.8\, K_{K,L} \dot{W}_{HX}(x_{3,\tau} - x_4) + 2.645\, U_{L,HX}(T_{g,in} - x_4)$$

Second-order temperature time delay:

$$x_{3,\tau} = x_3 + x_5$$

where

$$\dot{x}_5 = x_6 - \frac{12.0}{\tau} x_3$$

$$\dot{x}_6 = \frac{-12}{\tau^2} x_5 - \frac{6}{\tau} x_6 + \frac{72}{\tau^2} x_3$$

Argon gas temperature:

$$\dot{x}_7 = \frac{x_7}{2.88}\left[1.258\, K_{K,g}\dot{W}_g(T_{g,in} - x_7) + 1.99\, U_g(x_3 - x_7)\right]$$

The preceding seven equations can be written as follows,

$$\dot{X} = f(X, u)$$

Define

$$\rho_1 = 2.17\times10^{-4}$$

$$\rho_2 = -3.233\times10^{-3}$$

$$\rho_3 = -7.317\times10^{-6}$$

$$\rho_4 = 1.96\times10^{-2}$$

ρ_{in} = reactivity insertion

Then

$$\frac{\partial\delta k}{\partial x_2} = \frac{\rho_1}{x_2}$$

$$\frac{\partial\delta k}{\partial x_3} = 0.2\,\rho_2 x_3^{-0.8} + \frac{\rho_3}{2}$$

$$\frac{\partial\delta k}{\partial x_4} = \frac{\rho_3}{2}$$

From equation (B1), the elements of the first row of the coefficient matrix is determined. Note that all partial derivatives are evaluated at the design operating point (i.e., $X = X^o$ and $u = u^o$)

$$a_{11} = \frac{\partial\dot{x}_1}{\partial x_1} = \frac{\lambda\beta}{\beta - \delta k} - \lambda = \frac{\lambda\beta}{\beta} - \lambda = 0$$

$$a_{12} = \frac{\partial \dot{x}_1}{\partial x_2} = -\lambda\beta x_1^o(\beta - \delta k)^{-2}\left(-\frac{\partial \delta k}{\partial x_2}\right) = \frac{\lambda x_1^o}{\beta}\frac{\rho_1}{x_2^o}$$

$$a_{13} = \frac{\partial \dot{x}_1}{\partial x_3} = \frac{\lambda x_1^o}{\beta}\frac{\partial \delta k}{\partial x_3} = \frac{\lambda x_1^o}{\beta}\left[0.2\,\rho_2(x_3^o)^{-0.8} + \frac{\rho_3}{2}\right]$$

$$a_{14} = \frac{\partial \dot{x}_1}{\partial x_4} = \frac{\lambda x_1^o}{\beta}\frac{\partial \delta k}{\partial x_4} = \frac{\lambda x_1^o}{\beta}\frac{\rho_3}{2}$$

$$a_{15} = a_{16} = a_{17} = \frac{\partial \dot{x}_1}{\partial x_7} = 0$$

The remaining elements of the coefficient matrix are determined in the same manner as described

$$a_{21} = \frac{\partial \dot{x}_2}{\partial x_1} = 9.88\,\frac{\lambda l^*}{\beta}$$

$$a_{22} = \frac{\partial \dot{x}_2}{\partial x_2} = -2.398\,U_{L,C} + 9.88\,\frac{\lambda l^* x_1^o}{\beta^2}\frac{\partial \delta k}{\partial x_2}$$

$$a_{23} = \frac{\partial \dot{x}_2}{\partial x_3} = 2.398\,U_{L,C} + 9.88\,\frac{\lambda l^* x_1^o}{\beta^2}\frac{\partial \delta k}{\partial x_3}$$

$$a_{24} = \frac{\partial \dot{x}_2}{\partial x_4} = \frac{9.88\lambda l^* x_1^o}{\beta^2}\frac{\partial \delta k}{\partial x_4}$$

$$a_{25} = a_{26} = a_{27} = 0$$

$$a_{31} = 0$$

$$a_{32} = 10.37\,U_{L,C}$$

$$a_{33} = -42.5\,\dot{W} - 10.37\,U_{L,C}$$

$$a_{34} = 42.5\,\dot{W}$$

$$a_{35} = a_{36} = a_{37} = 0$$

$$a_{41} = a_{42} = 0$$

$$a_{43} = \frac{\partial \dot{x}_4}{\partial x_3} = 11.8\ K_{K,L} \dot{W}_{HX}$$

$$a_{44} = \frac{\partial \dot{x}_4}{\partial x_4} = -\ 11.8\ K_{K,L} \dot{W}_{HX} - 2.645\ U_{L,HX}$$

$$a_{45} = \frac{\partial \dot{x}_4}{\partial x_5} = 11.8\ K_{K,L} \dot{W}_{HX}$$

$$a_{46} = a_{47} = 0$$

$$a_{51} = a_{52} = a_{54} = a_{57}$$

$$a_{53} = \frac{\partial \dot{x}_5}{\partial x_3} = \frac{-12}{\tau}$$

$$a_{55} = \frac{-12}{\tau^2}$$

$$a_{56} = \frac{-6}{\tau}$$

$$a_{61} = a_{62} = a_{64} = a_{67} = 0$$

$$a_{63} = \frac{72}{\tau^2}$$

$$a_{65} = \frac{-12}{\tau^2}$$

$$a_{66} = \frac{-6}{\tau}$$

$$a_{71} = a_{72} = a_{74} = a_{75} = a_{76} = 0$$

$$a_{73} = \frac{\partial \dot{x}_7}{\partial x_3} = \frac{1.99}{2.88} U_g x_7^o$$

$$a_{77} = \frac{\partial \dot{x}_7}{\partial x_7} = \frac{x_7^o}{2.88}\left[-1.258\, K_{K,g}\dot{W}_g - 1.99\, U_g + 1.99\, x_3^o - x_7^o \frac{\partial u_g}{\partial x_7}\right]$$
$$+ \frac{1}{2.88}\left[1.258\, K_{K,g}\dot{W}_g\left(T_{g,in} - x_7^o\right) + 1.99\, U_g\left(x_3^o - x_7^o\right)\right]$$

$$U_g = \left(h_g^{-1} + 0.46\right)^{-1}$$

$$h_g = 4.08\, \dot{W}_g^{0.8}\left(-1.25\times10^{-9}\, x_7^2 + 5.75\times10^{-6}\, x_7 + 1.45\times10^{-2}\right)$$

$$\frac{\partial U_g}{\partial x_7} = \frac{h_g^{-2}}{\left(h^{-1} + 0.46\right)^2}\frac{\partial h_g}{\partial x_7} = \frac{U_g^2}{h_g^2}\frac{\partial h_g}{\partial x_7}$$

$$\frac{\partial h_g}{\partial x_7} = 4.08\, \dot{W}_g^{0.8}\left(-2.5\times10^{-9}\, x_7^o + 5.75\times10^{-6}\right)$$

The elements of the input matrix are determined in the same manner as the coefficient matrix.

Reactivity input disturbance:

$$b_1 = \frac{\partial \dot{x}_1}{\partial \rho_{in}} = \frac{\lambda x_1^o}{\beta}\frac{\partial \delta k}{\partial \rho_{in}} = \frac{\lambda x_1^o}{\beta}$$

$$b_2 = \frac{\partial \dot{x}_2}{\partial \rho_{in}} = \frac{9.88\lambda l^* x_1^o}{\beta^2}\frac{\partial \delta k}{\partial \rho_{in}} = \frac{9.88\lambda l^* x_1^o}{\beta^2}$$

$$b_3 = b_4 = b_5 = b_6 = b_7 = 0$$

Argon flow rate disturbance:

$$b_1 = b_2 = b_3 = b_5 = b_6 = 0$$

$$b_4 = \frac{\partial \dot{x}_4}{\partial \dot{W}_g} = 11.8\ \dot{W}_{HX}\left(x_5^o + x_3^o - x_4^o\right)\frac{\partial K_{K,L}}{\partial \dot{W}_g} + 2.645\left(T_{g,in} - x_4^o\right)\frac{\partial U_{L,HX}}{\partial \dot{W}_g}$$

$$K_{K,L} = -0.5443\ \dot{W}_g + 0.2817$$

$$U_{L,HX} = \left(1.13\ h_{g,in}^{-1} + \frac{1}{h_{L,HX}} + 0.46\right)^{-1}$$

$$h_{g,in} = 8.33\times10^{-2}\ \dot{W}_g^{0.8}$$

$$\frac{\partial K_{K,L}}{\partial \dot{W}_g} = -0.5443$$

$$\frac{\partial u_{L,HX}}{\partial \dot{W}_g} = U_{L,HX}^2\ \frac{1.13}{h_{g,in}^2}\ \frac{\partial h_{g,in}}{\partial \dot{W}_g}$$

$$\frac{\partial h_{g,in}}{\partial \dot{W}_g} = 6.66\times10^{-2}\ W_g^{-0.2}$$

$$b_7 = \frac{\partial \dot{x}_7}{\partial \dot{W}_g} = \frac{x_7^o}{2.88}\left[1.258(T_{g,in} - x_7^o\left(K_{K,g} + \dot{W}_g\ \frac{\partial K_{K,g}}{\partial \dot{W}_g}\right) + 1.99\left(x_3^o - x_7^o\right)\frac{\partial U_g}{\partial \dot{W}_g}\right]$$

$$K_{K,g} = 0.219\ \dot{W}_g + 0.0366$$

$$U_g = \left(h_g^{-1} + 0.46\right)^{-1}$$

$$h_g = 4.08\ \dot{W}_g^{0.8}\left(-1.25\times10^{-9}\ x_7^2 + 5.75\times10^{-6}\ x_7 + 1.45\times10^{-2}\right)$$

$$\frac{\partial K_{K,g}}{\partial \dot{W}_g} = 0.219$$

$$\frac{\partial U_g}{\partial \dot{W}_g} = \frac{U_g^2}{h_g^2} \frac{\partial h_g}{\partial \dot{W}_g}$$

$$\frac{\partial h_g}{\partial \dot{W}_g} = 3.26\, \dot{W}_g^{-0.2} \left(-1.25\times10^{-9}\, x_7^o \cdot x_7^o + 5.75^{-6}\, x_7^o + 1.45\times10^{-2}\right)$$

REFERENCES

1. Melsa, James L.: A Digital Computer Program for the Analysis and Design of State Variable Feedback Systems. NASA CR-850, 1967.

2. Turney, George; Kieffer, Arthur W.; and Petrik, Edward: Operating Characteristics of the Preliminary Flow Loop of a Conceptual Nuclear Brayton Powerplant. NASA TM X-2161, 1971.

3. Glasstone, Samuel; and Sesonske, Alexander: Nuclear Reactor Engineering. D. Van Nostrand Co., Inc., 1963.

4. Schultz, Donald G.; and Melsa, James L.: State Functions and Linear Control Systems. McGraw-Hill Book Co., Inc., 1967.

5. Weaver, Lynn E.: System Analysis of Nuclear Reactor Dynamics. Rowman & Littlefield, Inc., 1963.

TABLE I. - DESIGN POINT OPERATING CONDITIONS

Reactor thermal power, Q, MW_t	2.17
Lithium temperature at reactor inlet (or heat exchanger exit), ^{o}R (K)	2100 (1167)
Lithium temperature at reactor exit (or heat exchanger inlet), ^{o}R (K)	2200 (1222)
Lithium flow rate, $\dot{W}_L$, lbm/sec (kg/sec)	20.7 (9.39)
Argon temperature at heat exchanger inlet, ^{o}R (K)	1560 (867)
Argon temperature at heat exchanger exit, ^{o}R (K)	2060 (1144)
Argon flow rate, $\dot{W}_g$, lbm/sec (kg/sec)	32.8 (14.88)

TABLE II. - DECAY CONSTANTS AND YIELD FRACTIONS

OF DELAYED-NEUTRON PRECURSORS -

FAST FISSION U^{235}

Group	Decay constant, λ_i, sec^{-1}	Yield fraction, β_i
1	3.8800	0.0001719
2	1.4000	.0008430
3	.3110	.0026900
4	.1160	.0012380
5	.0317	.0014020
6	.0127	.0002520

TABLE III. - NUCLEAR BRAYTON SPACE POWERPLANT DESCRIPTION AND SIMPLIFYING

ASSUMPTIONS OF THE NONLINEAR DIFFERENTIAL EQUATIONS

Case	Reactor kinetics	Reactor heat transfer	Heat exchanger heat transfer
Original simulation	Six neutron groups	Three axial segments including cladd, fuel, and lithium temperatures	Three axial segments including argon gas, wall, and lithium temperatures
Case A	One delayed neutron group	Same as original simulation	Same as original simulation
Case B	One delayed neutron group	One axial segment including cladd, fuel, and lithium temperatures	One axial segment including argon gas, wall, and lithium temperatures
Case C	One delayed neutron group	One axial segment including fuel and lithium temperatures, i.e., temperature of lithium to clad assumed zero	One axial segment including argon gas, and lithium temperature, i.e., temperature of lithium to wall assumed zero
Case D	One delayed neutron group	Same as case C	Same as case B

TABLE IV. - SUMMARY OF TIME RESPONSE FOR VARIOUS STEP DISTURBANCES

Variable	Original simulation					Transfer function approximation				
	Peak overshoot		Time of peak, sec	Final value		Peak overshoot		Time of peak, sec	Final value	
	°R	K		°R	K	°R	K		°R	K
Reactivity step, 1 cent										
Reactor fuel temperature	11.2	6.2	103	8.7	4.8	13.1	7.3	105	9.4	5.2
Reactor exit lithium temperature	9.6	5.3	122	7.7	4.3	11.2	6.2	117	8.2	4.6
Reactor inlet lithium temperature	8.0	4.4	153	6.5	3.6	9.4	5.2	133	7.0	3.9
Argon temperature	7.6	4.2	132	6.2	3.4	8.8	4.9	119	6.5	3.6
Argon flow rate, 5 percent										
Reactor fuel temperature	-2.1	-1.2	34	4.8	2.7	-3.2	-1.8	29	6.4	3.6
Reactor exit lithium temperature	-4.0	-2.2	51	1.2	.7	-5.5	-3.1	42	2.0	1.1
Reactor inlet lithium temperature	-7.6	-4.2	78	-3.4	-1.9	-9.0	-5.0	57	-2.6	-1.4
Argon temperature	-6.2	-3.4	61	-2.2	-1.2	-7.6	-4.2	42	-1.7	-.9
Lithium flow rate step, 25 percent										
Reactor fuel temperature	-6.8	-3.8	3.1	-1.2	-.7	-10.9	-6.1	3.8	-8.6	-4.8
Reactor exit lithium temperature	-14.1	-7.8	2.6	-7.0	-3.9	-12.7	-7.1	1.9	-8.5	-4.7
Reactor inlet lithium temperature	13.4	7.4	12.0	13.1	7.3	11.9	6.6	8.0	11.5	6.4
Argon temperature	-3.2	-1.8	2.0	-1.0	-.6	-7.5	-4.2	1.9	-4.1	-2.3

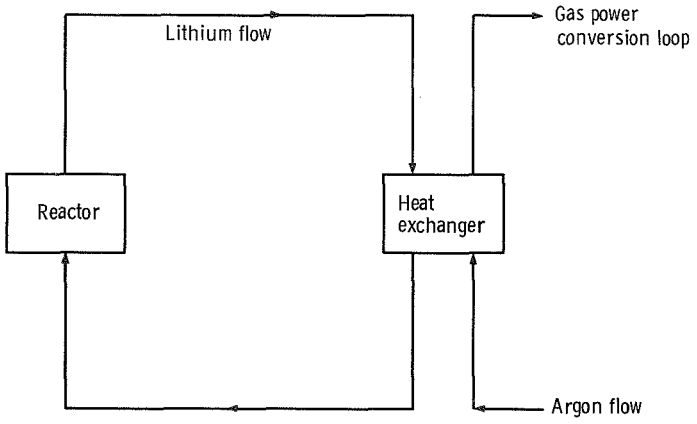

Figure 1. - Primary loop of nuclear Brayton space powerplant.

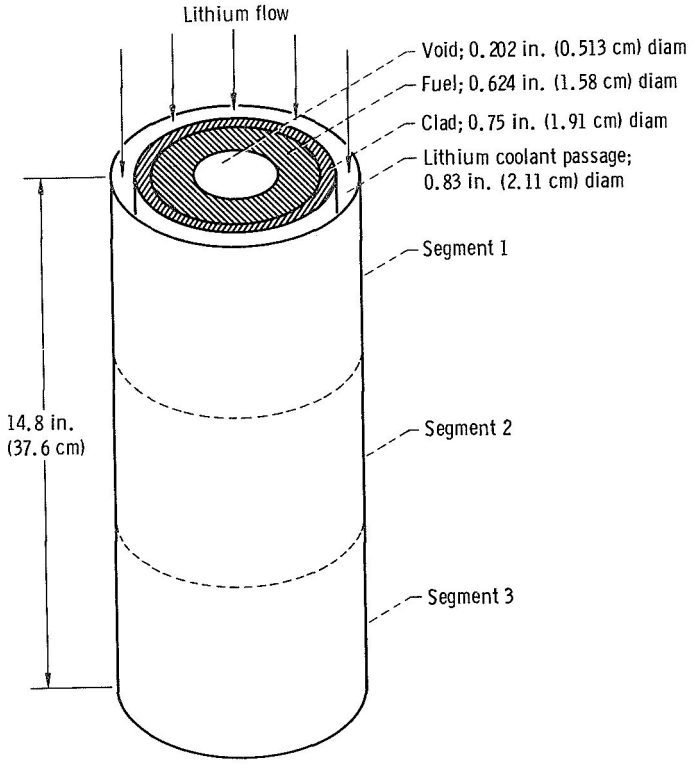

Figure 2. - Single fuel pin model of reactor core (not to scale).

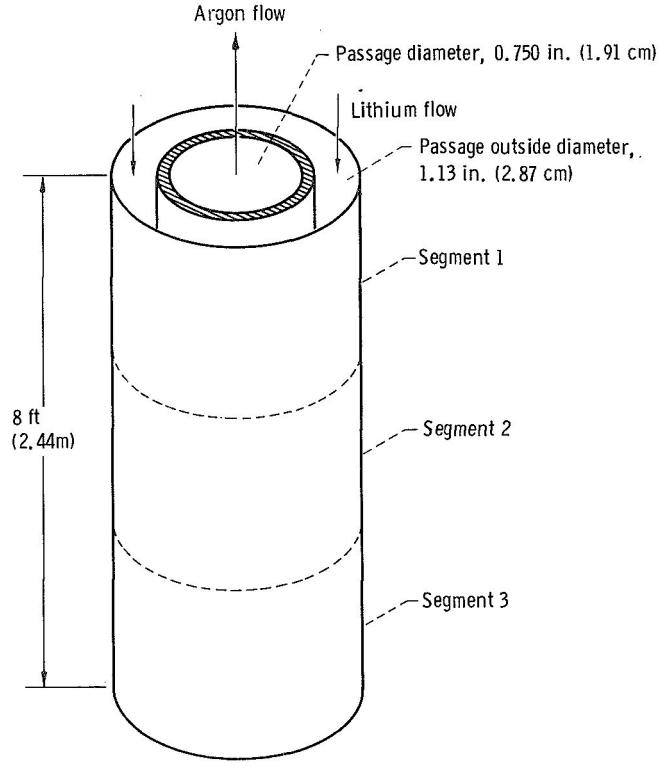

Figure 3. - Single tube model of shell-and-tube heat exchanger (not to scale).

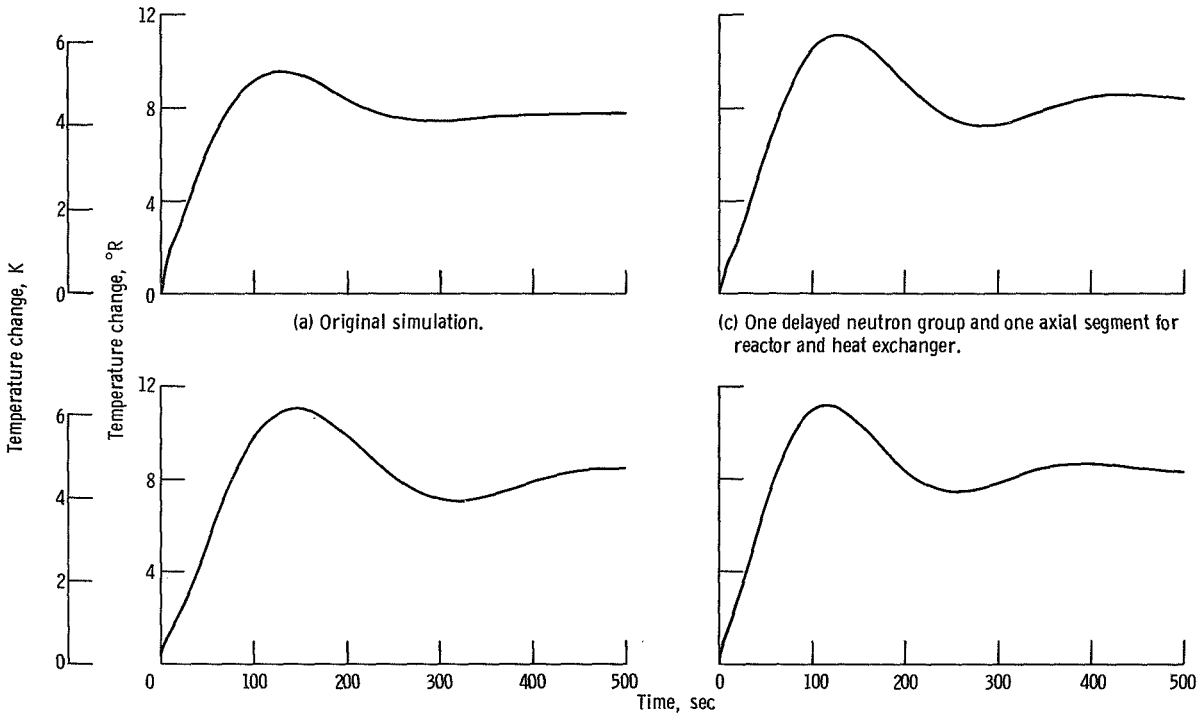

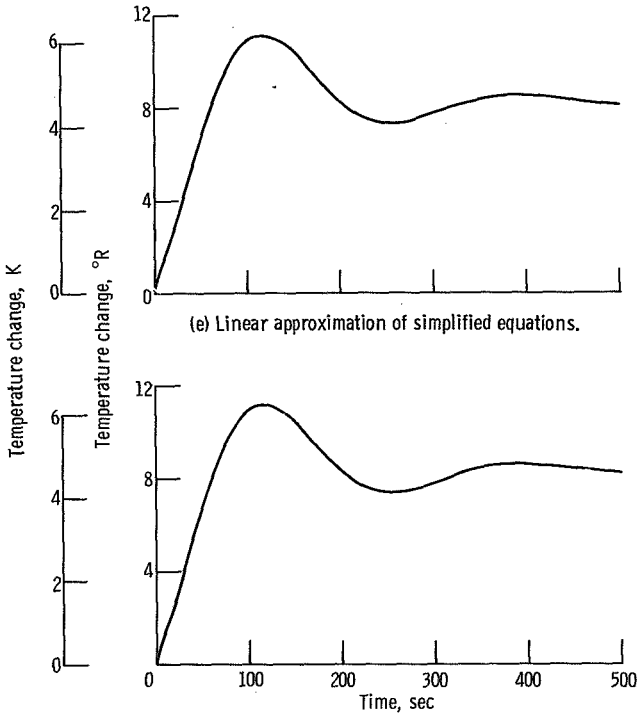

Figure 4. - Time response about design operating point of reactor exit lithium temperature to 1-cent step disturbance in reactivity.

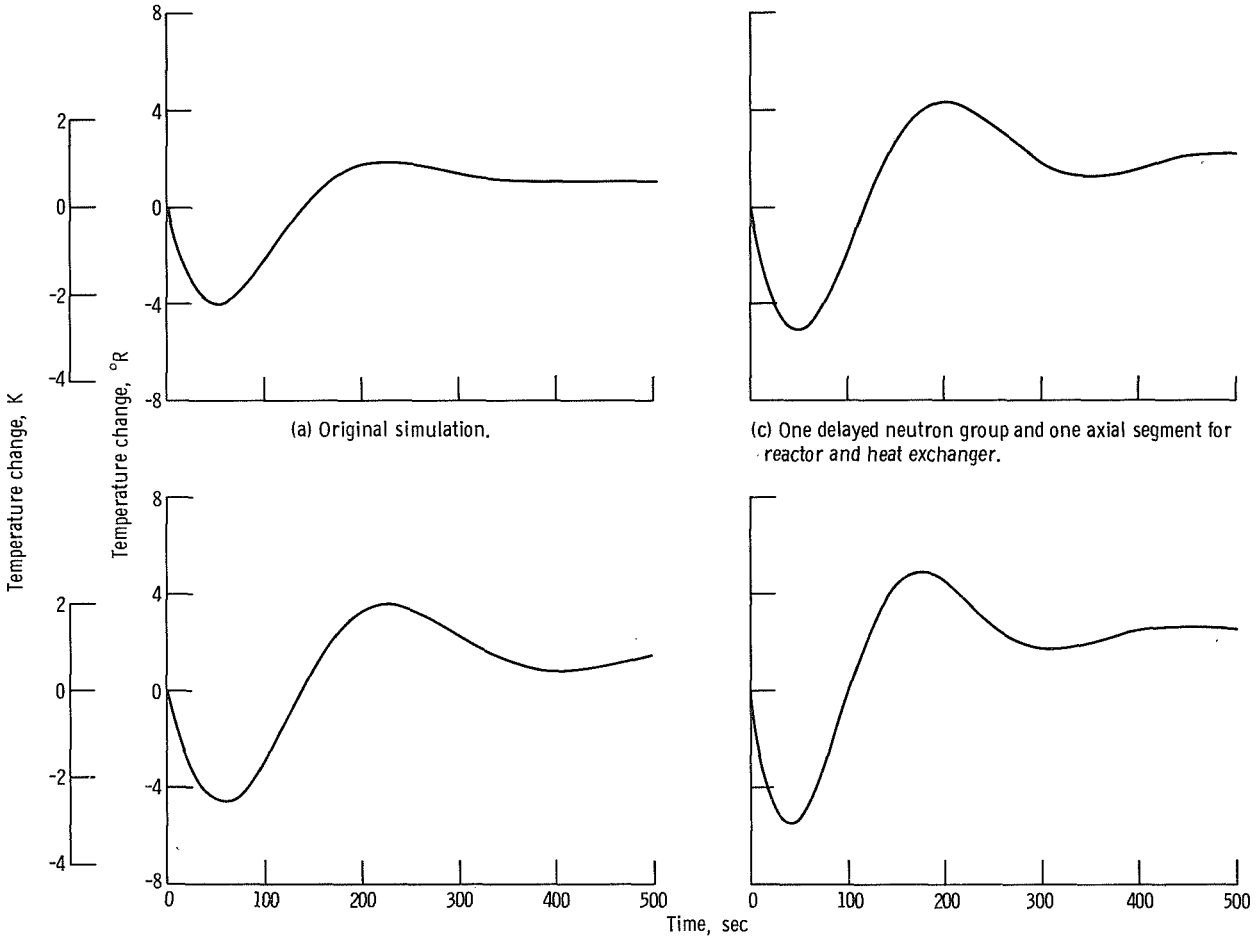

Figure 5. - Time response about design operating point of reactor exit lithium temperature to 5-percent step disturbance in argon flow rate.

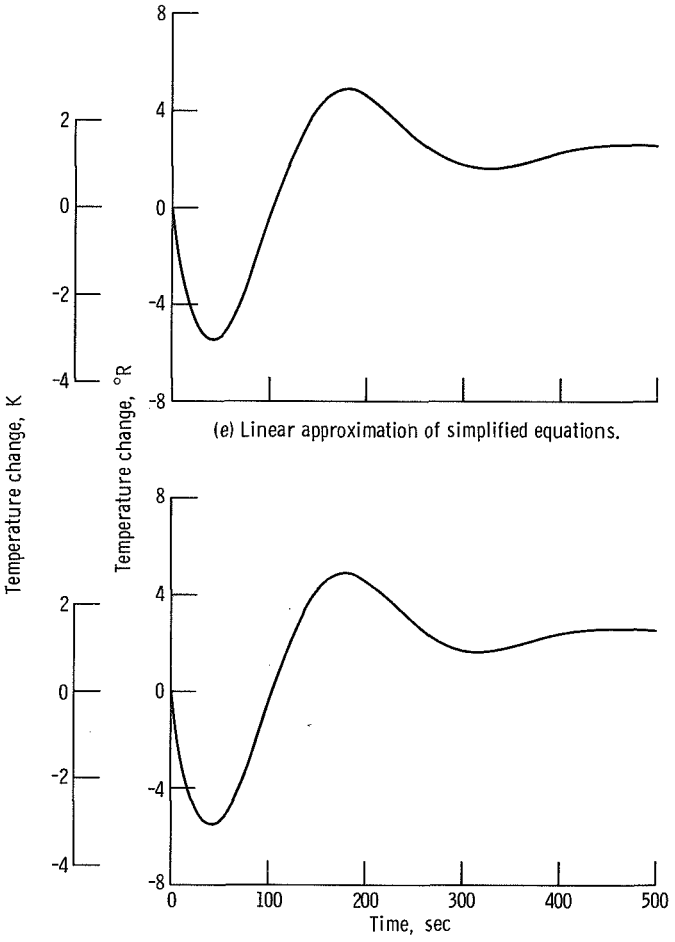

(e) Linear approximation of simplified equations.

(f) Inverse Laplace transform.

Figure 5. - Concluded.

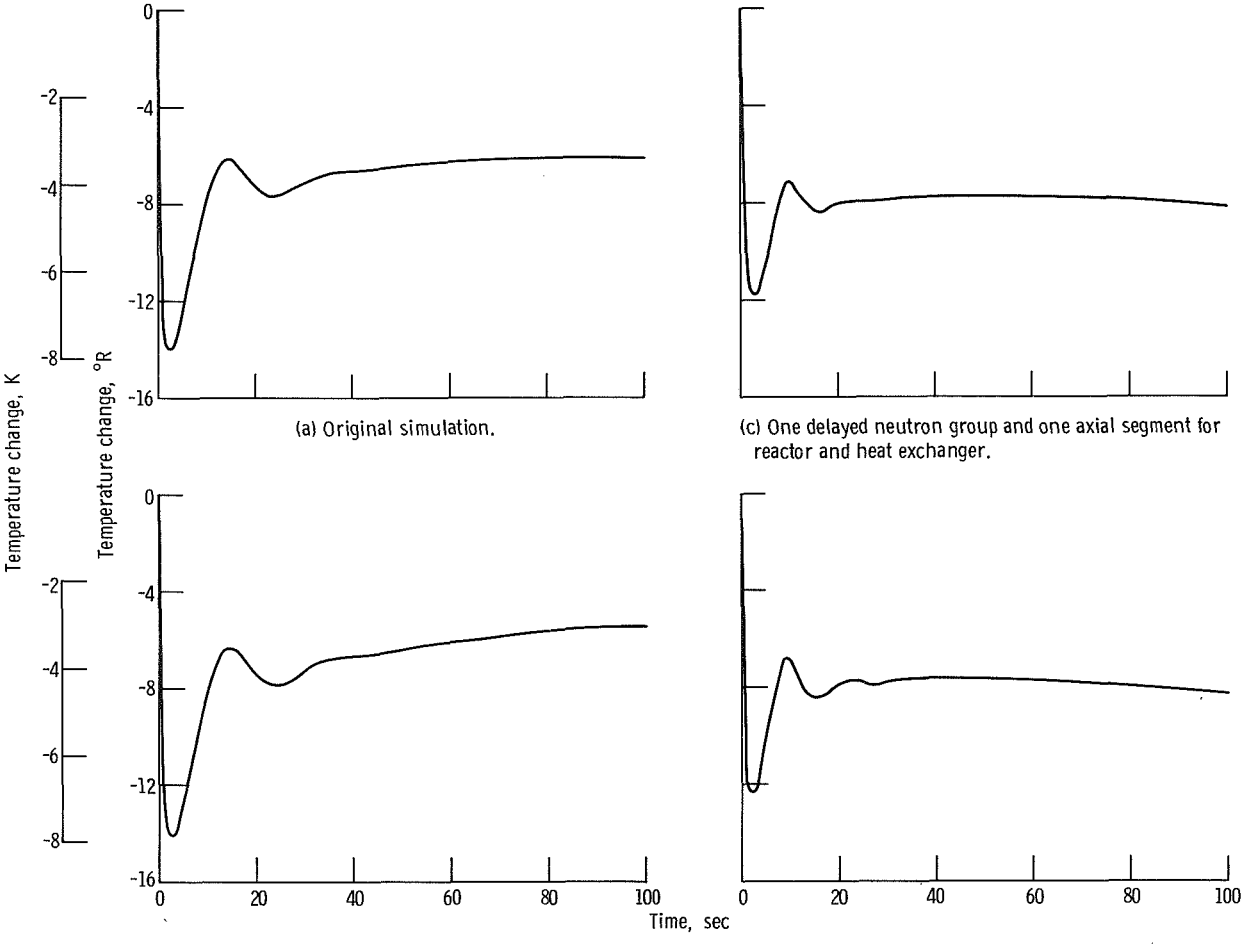

(a) Original simulation.

(b) One delayed neutron group and three axial segments for reactor and heat exchanger.

(c) One delayed neutron group and one axial segment for reactor and heat exchanger.

(d) One delayed neutron group and one axial segment with delta temperature of lithium to wall assumed to be zero..

Figure 6. - Time response about design operating point of reactor exit lithium temperature to 25-percent step disturbance in lithium flow rate.

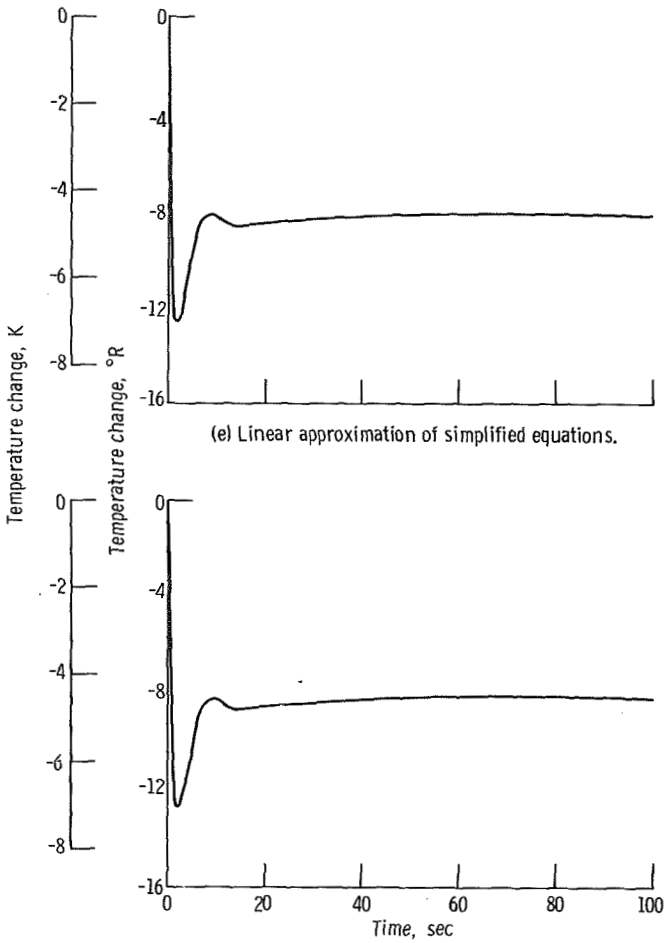

(e) Linear approximation of simplified equations.

(f) Inverse Laplace transform.

Figure 6. - Concluded.

NASA-Langley, 1971 — 22 E-5830

NATIONAL AERONAUTICS AND SPACE ADMINISTRATION
WASHINGTON, D.C. 20546

OFFICIAL BUSINESS

FIRST CLASS MAIL

POSTAGE AND FEES PAID
NATIONAL AERONAUTICS A
SPACE ADMINISTRATION

POSTMASTER

"The aeronautical and space activities of the United States shall be conducted so as to contribute . . . to the expansion of human knowledge of phenomena in the atmosphere and space. The Administration shall provide for the widest practicable and appropriate dissemination of information concerning its activities and the results thereof."

— NATIONAL AERONAUTICS AND SPACE ACT OF 1958

NASA SCIENTIFIC AND TECHNICAL PUBLICATIONS

TECHNICAL REPORTS: Scientific and technical information considered important, complete, and a lasting contribution to existing knowledge.

TECHNICAL NOTES: Information less broad in scope but nevertheless of importance as a contribution to existing knowledge.

TECHNICAL MEMORANDUMS: Information receiving limited distribution because of preliminary data, security classification, or other reasons.

CONTRACTOR REPORTS: Scientific and technical information generated under a NASA contract or grant and considered an important contribution to existing knowledge.

TECHNICAL TRANSLATIONS: Information published in a foreign language considered to merit NASA distribution in English.

SPECIAL PUBLICATIONS: Information derived from or of value to NASA activities. Publications include conference proceedings, monographs, data compilations, handbooks, sourcebooks, and special bibliographies.

TECHNOLOGY UTILIZATION PUBLICATIONS: Information on technology used by NASA that may be of particular interest in commercial and other non-aerospace applications. Publications include Tech Briefs, Technology Utilization Reports and Technology Surveys.

Details on the availability of these publications may be obtained from:

SCIENTIFIC AND TECHNICAL INFORMATION OFFICE

NATIONAL AERONAUTICS AND SPACE ADMINISTRATION

Washington, D.C. 20546